Terahertz Radiation from InAs with Various Surface Orientations under Magnetic Field Irradiated with Femtosecond Optical Pulses at Different Wavelengths

doi: 10.1063/1.1690099

Terahertz radiation from InAs with various surface orientations under magnetic field irradiated with femtosecond optical pulses at different wavelengths

Hiroshi Takahashi[a)]
Department of Photo Science, The Graduate University for Advanced Studies, Shonan Village, Hayama 240-0193, Japan

Masahiro Sakai, Alex Quema, Shingo Ono,[b)] and Nobuhiko Sarukura[b)]
Institute for Molecular Science (IMS), Myodaiji, Okazaki 444-8585, Japan

Gen Nishijima and Kazuo Watanabe
High Field Laboratory for Superconducting Materials, Institute for Materials Research, Tohoku University, Katahira, Aoba-ku, Sendai 980-8577, Japan

(Received 3 November 2003; accepted 4 February 2004)

We present the magnetic-field dependence of terahertz (THz)-radiation power from femtosecond-laser-irradiated InAs with various surface orientations. Under 800 nm optical excitation, the magnetic field that provides the maximum THz-radiation power is found to be affected by the surface orientation, and InAs (111) exhibits it at lower magnetic fields than that of the other surfaces. In contrast, under 1560 nm excitation, the dependence on the surface orientation almost disappeared, and saturation is observed at a much smaller magnetic field than that in the 800 nm excitation case. Additionally, from the results of magnetic-field dependence up to 14 T, the shift of the peak in the THz-radiation spectrum toward lower frequency is confirmed, depending on the magnetic field applied, which is possibly induced by the emergence of a magnetoplasma effect. © *2004 American Institute of Physics.* [DOI: 10.1063/1.1690099]

I. INTRODUCTION

Due to the rapid progress of ultrafast laser technology, much pioneering work has been done in various fields, not only in conventional physics but also in biophysics or medical sciences. This is due to the fact that an ultrafast laser is capable of producing high-rate stable optical pulse trains with sufficiently high-peak power, which is vital for ultrafast spectroscopy or material processing. To extend its area of activity, a great deal of attention has been focused on the findings of new research in conjunction with high-field physics in the terahertz (THz) regime including static electric fields or magnetic fields. As part of this, the semiconductor surface irradiated by ultrashort optical pulses is extensively studied under the effect of high magnetic field, since it is reported to generate electromagnetic waves in the far-infrared region, particularly in the THz frequency domain.

To generate THz radiation with high temporal coherence, various schemes have been demonstrated utilizing ultrashort optical pulses, including photoconductive switches,[1] semiconductor surfaces,[2] or nonlinear optical processes.[3,4] Among these techniques, use of an InAs surface is widely accepted as the practical THz radiation source since it provides intense THz radiation and it does not require chemical processes and microfabrication techniques for sample preparation. The physical origin of THz radiation from the semiconductor surface can be categorized into two major processes, difference-frequency mixing and transient photocurrent induced by photoexcitation. The former process creates instantaneous polarization via optical rectification, which is described by a second-order nonlinear susceptibility and becomes dominant under high-excitation conditions.[5,6] THz radiation originating from this process is reported to be significantly enhanced by using a (111) surface, since it has an asymmetric structure and nonlinear optical processes are effectively enhanced. In contrast, under low-excitation conditions, the contribution by transient photocurrent becomes the dominant source for THz radiation. The origin of transient photocurrent is classified in two ways depending upon the surface properties: the acceleration of photoexcited carriers by the surface-electric field, and the surge of current induced by different diffusion velocities between photoexcited electrons and holes. By exciting narrow-band gap semiconductors, e.g., InAs and InSb with near-infrared lasers, the latter process is thought to be the main source for THz radiation. This is because diffusion is significantly enhanced by both the narrow absorption depth and high kinetic energy of photoexcited carriers.[7–9]

Since Zhang *et al.* reported the quadratic magnetic-field dependence of THz-radiation power from GaAs,[10] many studies have shown that the application of a magnetic field causes an order of magnitude enhancement of THz radiation from various semiconductor surfaces.[11,12] This enhancement is explained by the change in direction of carrier acceleration, which is induced by Lorentz force in a magnetic field.[13–19] Because of the high contrast of the refractive index

[a)]Author to whom correspondence should be addressed; electronic mail: htakahas@ims.ac.jp
[b)]Also at Department of Photo Science, The Graduate University for Advanced Studies, Shonan Village, Hayama 240-0193, Japan.

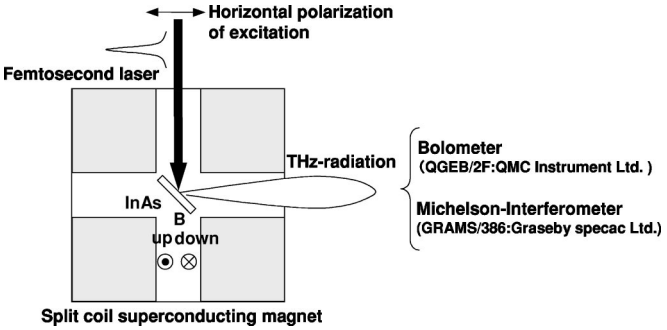

FIG. 1. Experimental setup for the THz-radiation emitter in a magnetic field. A Ti:sapphire laser and a fiber laser (IMRA model A50) were used as excitation sources. The laser spot size on sample surface was about 2 mm. The samples were undoped bulk InAs with (100), (110), and (111) surfaces. A liquid-helium-cooled Ge bolometer was used to detect the power of the total radiation. A magnet field was applied parallel to the sample surface. The maximum magnetic field of a split-coil superconducting magnet was 5 T.

at the semiconductor surface, the change of acceleration direction enhances the THz radiation transmitted through the air–semiconductor interface.[13] Previously, we achieved significant enhancement of THz-radiation power by using InAs and reported the quadratic magnetic-field and excitation intensity dependence of THz-radiation power.[20,21] Furthermore, anomalous magnetic-field dependence of THz-radiation power has been observed, including saturation, decrease, and recovery.[22,23] However, the physical mechanism for such magnetic-field dependence has still not been clarified, partly due to the lack of experimental results to provide clear insight with which to explore it.

This article presents the magnetic-field dependence of THz-radiation power from InAs with different surface orientations. The magnetic-field dependence of THz-radiation power exhibits a clear difference depending on the excitation wavelength and surface orientation. Under 800 nm optical excitation, magnetic-field dependence is affected by surface orientation. Compared to the (100) or (110) surface, InAs (111) exhibits significant deviation from quadratic magnetic-field dependence and its saturation point is dramatically shifted toward lower magnetic field. In contrast, for 1560 nm excitation, this shift is significantly enhanced, while the dependence on surface orientation almost disappears. A possible explanation for these results is briefly discussed by considering the effect of the nonparabolic band structure for InAs. Moreover, we investigated the magnetic-field dependence of THz-radiation power up to 14 T. The shift of the peak in the THz-radiation spectrum is clearly observed by applying a magnetic field, which might be related to the emergence of the magnetoplasma effect.

II. EXPERIMENT

The experimental setup for the THz-radiation emitter in a magnetic field is shown in Fig. 1. A Ti:sapphire laser and a fiber laser (IMRA model A50) were used as excitation sources. A mode-locked Ti:sapphire laser delivered 100 fs pulses at wavelengths from 775 to 850 nm with a 82 MHz repetition rate. A mode-locked fiber laser delivered 100 fs

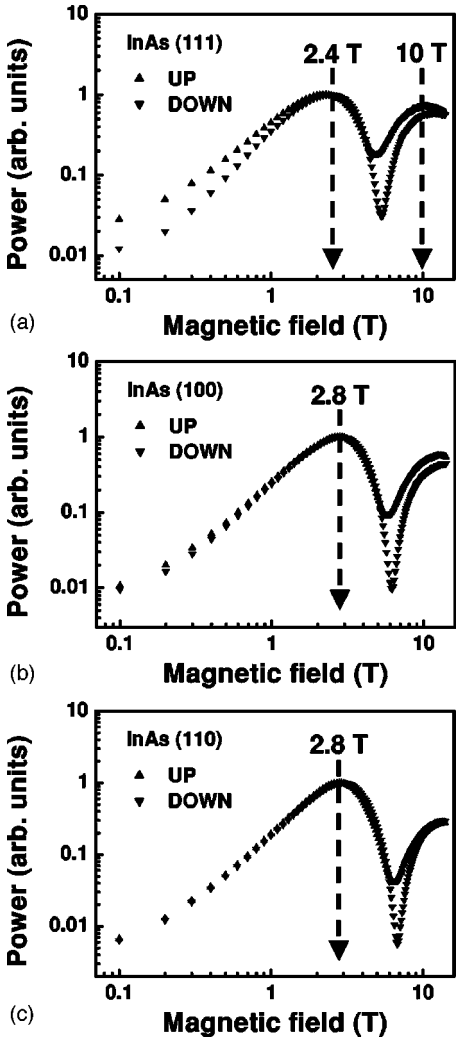

FIG. 2. Magnetic-field dependence of THz-radiation power. (a) InAs (111), (b) InAs (100), and (c) InAs (110) surfaces are irradiated with a femtosecond laser under excitation of 300 mW at a center wavelength of 800 nm.

pulses at a wavelength of 1560 nm with a 50 MHz repetition rate. The laser was *p* polarized and the laser spot size on the sample surface was approximately 2 mm. The samples were undoped bulk InAs with (100), (110), and (111) surfaces, which have carrier concentrations of 2.0×10^{16}, 2.0×10^{16}, and 1.85×10^{16} cm^{-3}, respectively. The doping densities of the InAs samples were measured by Hall measurement at room temperature. Magnetic fields were provided by a split-coil superconducting magnet and a cryogen-free superconducting magnet,[24] which are capable of producing maximum magnetic field up to 5 and 15 T, respectively. A liquid-helium-cooled Ge bolometer was used to detect the radiation power. The magnet field was applied parallel to the sample surface and perpendicular to the plane of incidence of the excitation laser. The THz-radiation spectrum was measured by a polarized Michelson interferometer.

III. RESULTS AND DISCUSSION

Figure 2 presents the magnetic-field dependence of THz radiation power from InAs with various surface orientations. For InAs (100), the THz radiation power exhibits quadratic

dependence on the magnetic field, and increases up to a saturation point at around 2.8 T. Then, the THz-radiation power decreases and reaches a minimum. By further increasing the magnetic field, the radiation power recovers and again saturates at around 13 T. For the (110) surface, magnetic-field dependence is quite similar to that of (100) surface, except that a small difference is observed in the saturation points. However, for the (111) surface, a significant difference is observed. The saturation point is observed at around 2.4 and 10 T, smaller than that for other surfaces. As reported by many researchers, the main mechanism for magnetic-field induced enhancement of THz-radiation power is considered to be caused by Lorentz force, which rotates the carrier acceleration toward the surface's parallel direction. The change of dipole direction leads to the enhancement of THz radiation due to dielectric contrast between air and the semiconductor surface.[13] This is observed in the experimental results below 2.8 T. The reduction of the THz-radiation power above 2.8 T is still under discussion. However, one possible explanation is given by the higher cyclotron frequency at magnetic field over 2.8 T, which leads to a smaller cyclotron radius so these dipoles cannot effectively contribute to generate THz radiation.

Figure 3 illustrates the excitation-wavelength dependence of THz-radiation power at various magnetic fields. A shift of the saturation point toward lower magnetic field is observed by varying the excitation wavelength from 775 to 850 nm. Under 1560 nm excitation, this shift is significantly enhanced, and observed at around 1.2 T independent of the surface orientation. We confirmed that the magnetic-field dependence of the THz-radiation power does not exhibit any difference with variation of the excitation power from 30 to 600 mW. This proves that the photoexcited carrier density cannot affect the magnetic-field dependence of THz-radiation power under the current experimental conditions, and the above phenomenon should be explained by the difference in excitation wavelength.

Figure 4 presents a schematic diagram of the band structure of InAs. During optical excitation, electrons are excited from the heavy-hole, light-hole, and split-off-hole bands to the conduction band, and populate in three separate regions in k space. The photoexcited electrons mainly originated from the first two excitation processes, and are then redistributed via electron–hole interactions at the subpicosecond time scale.[25] The effective electron mass in a Γ valley is given as the curvature of the conduction band, and the effect of the nonparabolic structure becomes significant as the kinetic energy of the electrons increases. In this case, the effective electron mass becomes heavier than that of the Γ valley and depends on its kinetic energy.[26] For excitation at 800 nm (1.55 eV), photoexcited carriers have high kinetic energy that far exceeds that of the band gap of InAs (0.36 eV), and the effect of the nonparabolic band structure becomes significant. Since InAs has an asymmetric band structure in k space, this effect leads to the effective mass of photoexcited carriers depending on both the k-space direction and the kinetic energy. In contrast, for 1560 nm excitation (0.79 eV), the band structure of InAs is almost a parabolic structure. Therefore, the effective mass of photoexcited

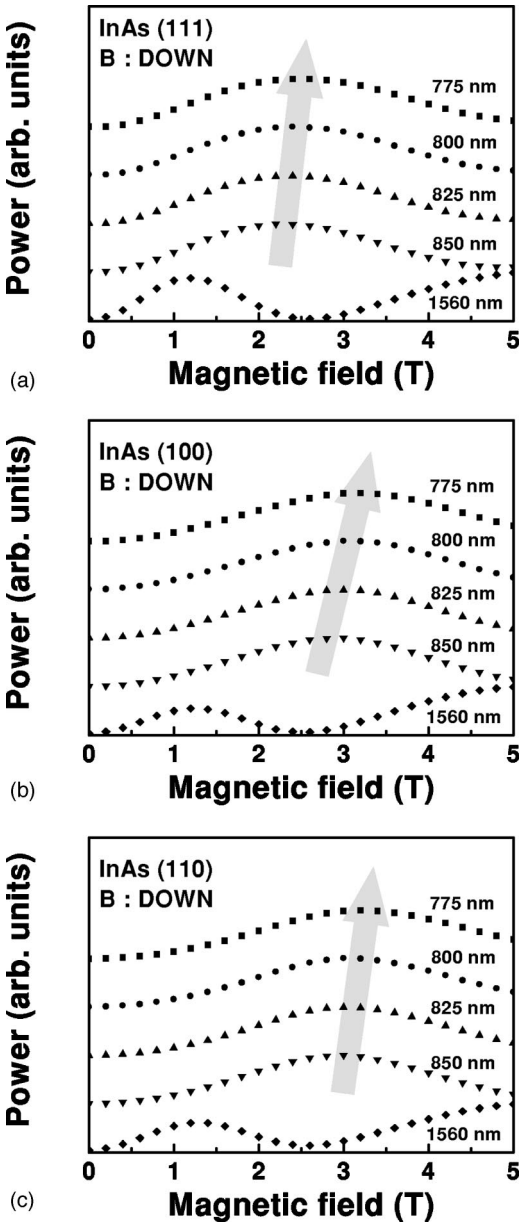

FIG. 3. Excitation-wavelength dependence of the THz-radiation power in varying magnetic fields. (a) InAs (111), (b) InAs (100), and (c) InAs (110) surfaces are irradiated with a femtosecond laser under excitation of 300 mW at wavelengths from 775 to 850 nm, and 160 mW at 1560 nm.

carriers is independent of the k-space direction. To discuss the saturation point, depending on the effective mass of photoexcited carriers, we briefly review a physical model to give the emitted THz-radiation power reported in Ref. 11.

In the presence of an external magnetic field, the photoexcited carriers are accelerated by Lorentz force and their motion is expressed as

$$m^*(d\boldsymbol{\nu}/dt) = -e(\mathbf{E} + \boldsymbol{\nu} \times \mathbf{B}), \tag{1}$$

where m^*, E, and B are the effective electron mass, surface electric field, and magnetic field applied, respectively. Here, we neglect motion of the holes, since their effective mass is much heavier than that of electrons. Assuming the surface electric field E points along the z axis and the magnetic field

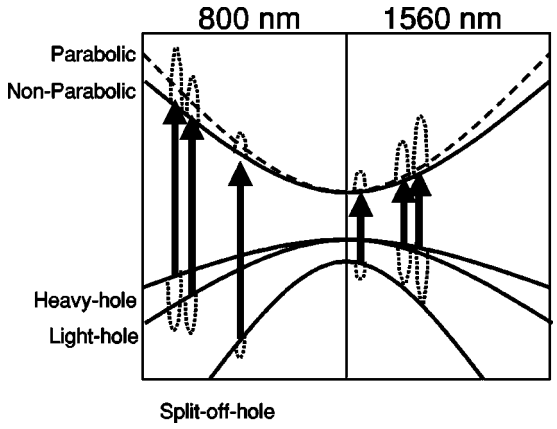

FIG. 4. Schematic diagram of the band structure of InAs. The excitation process is indicated by arrows that point upward. The valence band is composed of three bands, the heavy-hole, light-hole, and split-off-hole bands.

points along the x axis as shown in Fig. 3, the time-dependent acceleration of carriers is given by

$$a_y(t) = \frac{E}{B}\omega_c \sin(\omega_c t), \tag{2}$$

$$a_z(t) = \frac{E}{B}\omega_c \cos(\omega_c t), \tag{3}$$

where ω_c is the cyclotron frequency.

For small magnetic fields, $\omega_c t$ is small, so the instantaneous THz electric field is expressed as

$$E_y \propto a_y(t) = \frac{E}{B}\omega_c^2 t = \left(\frac{e}{m^*}\right)^2 EBt \tag{4}$$

and

$$E_z \propto \frac{E}{B}\omega_c = \frac{eE}{m^*}, \tag{5}$$

where t is the acceleration time, which depends on the time it takes for the carriers to reach constant velocity. These equations mean that there are two components of carrier acceleration that can generate THz radiation. In this article, we measure the THz-radiation power enhanced by an external magnetic field. Therefore, we focus on the THz electric field given by Eq. (4). THz-radiation power is given as the time integral of Eq. (3) and expressed as

$$P_{\mathrm{THz}} \propto \int_0^{\tau} E_y^2 dt = \alpha B^2, \tag{6}$$

where τ is the average acceleration time and α is the scaling factor.

At small magnetic fields, the THz-radiation power exhibits quadratic magnetic-field dependence that follows Eq. (6). However, the linear approximation leading to Eqs. (4) and (5) is no longer valid at higher magnetic fields, and saturation of the THz-radiation power is expected to be observed at high magnetic field depending upon the effective mass of photoexcited electrons.

Figure 5 presents THz-radiation spectra of InAs measured at various magnetic fields. All spectra show consistent

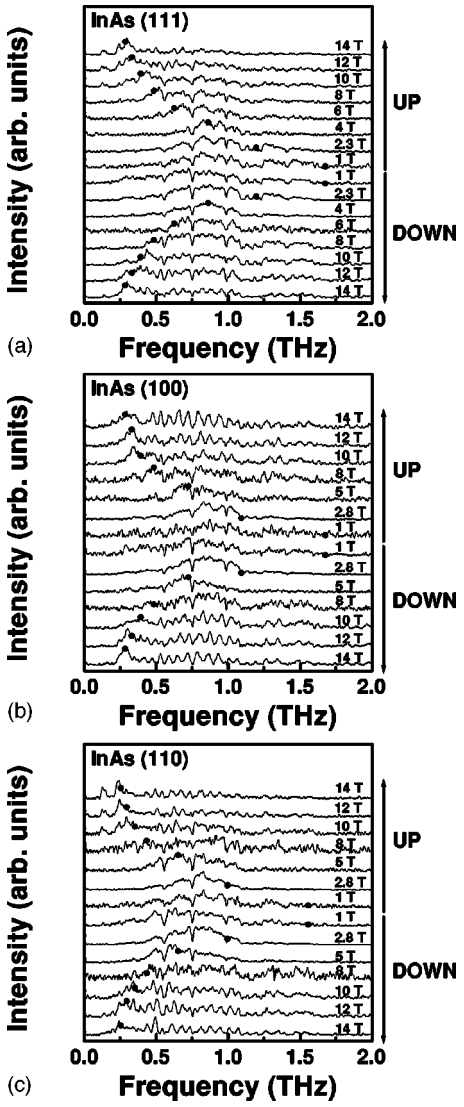

FIG. 5. THz-radiation spectra measured at magnetic fields up to 14 T. (a) InAs (111), (b) InAs (100), and (c) InAs (110) surfaces are irradiated with a femtosecond laser under excitation of 300 mW at a wavelength at 800 nm.

results. At magnetic fields below 5 T, the THz-radiation spectrum exhibits a broad band structure, and the low-frequency component is dramatically enhanced with an increase in magnetic field. At magnetic fields above 5 T, the peak frequency of the THz-radiation spectrum shifts toward the low-frequency side with an increase in magnetic field. Additionally, the periodic structure is observed in the THz-radiation spectrum at magnetic fields above 10 T. This is attributed to a change of dielectric constant induced by the strong magnetic field and results in interference of THz pulses from the front and back surfaces of the InAs substrate.[23] Kersting *et al.* investigated the THz radiation from an *n*-GaAs surface and reported that its origin can be ascribed to plasma oscillation of the extrinsic carriers in the bulk sample, which is initiated by screening of the surface depletion field.[27,28] Heyman *et al.* have extended this model to include magnetic-field effects.[16] They reported that THz radiation from the *n*-GaAs surface in a magnetic field could be described well by their model, whereas quantitative agreement of the peak frequency in the THz-radiation spectra is only achieved for

n-type InAs. In their experiment, they measured the magnetic-field dependence of the THz-radiation spectrum up to 5 T. To evaluate their model in more detail, we fitted it to the magnetic-field dependence of THz-radiation spectra at magnetic fields up to 14 T. In their model, the dynamics of a homogeneous three-dimensional plasma of charges in the shifted coordinate system are expressed as

$$\mathbf{a} = -\omega_p^2 \mathbf{r} - \frac{e\boldsymbol{\nu} \times \mathbf{B}}{m^*} - \gamma \boldsymbol{\nu}, \tag{7}$$

where ω_p is the plasma frequency, and γ is the effective scattering rate. For the case of the initial displacement and velocity of charge perpendicular to the magnetic field, the eigenvalues of magnetoplasma frequencies are given as

$$\omega_{\pm} = \frac{1}{2}[(\omega_c + i\gamma) \pm \sqrt{(\omega_c + i\gamma)^2 + 4\omega_p^2}], \tag{8}$$

where ω_c is the cyclotron frequency.[16] The calculated frequencies of the lower branch of the magnetoplasma for zero damping are shown as black circles in Fig. 5. In this calculation, the dielectric constant of InAs and the effective mass of extrinsic electrons were set at 11.8 and $0.024m_0$, respectively. At higher magnetic field, the peak frequency of the THz-radiation spectrum follows the calculated magnetoplasma frequencies, and shifts toward lower frequency with an increase in magnetic field. This implies that the origin of the new THz-radiation spectrum observed at magnetic fields above 5 T might be ascribed to the lower branch of the magnetoplasma. Here, it should be noted that the frequency bandwidth of the detection system is limited by the system response of the Michelson interferometer and is estimated to be around 2 THz. Therefore, the higher frequency components over 2 THz cannot be detected in the spectrum data. This idea is also supported by the periodic structure of the THz-radiation spectrum observed at higher magnetic fields, since the appearance of magnetoplasma can contribute to a change in both real and imaginary parts of the refractive index in the THz region. However, further investigation is required to validate this. A study of the THz-radiation spectrum of InAs with different doping densities may provide clearer results, since the magnetoplasma frequency shift toward the high frequency side depends upon the doping density of the InAs substrate.[29,30]

IV. CONCLUSION

We investigated the magnetic-field dependence of THz-radiation power from InAs with different surface orientations. We found that the magnetic-field dependence of THz-radiation power is affected by the surface orientation for the 800 nm excitation case, and that the maximum THz-radiation power from InAs (111) is obtained at magnetic field of around 2.4 T, which is lower than that of (100) and (110) surfaces. Under 1560 nm excitation, the shift of the saturation point is significantly enhanced, although the dependence upon the surface orientation almost disappeared. From the brief discussion of these experimental results, we want to point out that the effective electron mass plays an important role in the magnetic-field dependence of THz-radiation power and that the band structure of InAs, including the effect of the *k*-space direction and nonparabolic structure, must be taken into account when building a complete physical model. Moreover, we investigated the magnetic-field dependence of THz-radiation power up to 14 T. It is found that the peak frequency of the THz-radiation spectrum shifts toward the low-frequency side with an increase in magnetic field, which might be related to the lower branch of the magnetoplasma effect. The physical origin of these phenomena is still under discussion, however, our experimental results prove that there is a big possibility of coming across really exciting results in the field of ultrafast laser technology related to a high magnetic field.

ACKNOWLEDGMENTS

The authors thank Sugiura, Hirosumi, Dr. Ohtake, and Dr. Yoshida of AISIN Corp. for their encouragement of this work. This research was partially supported by a Sasakawa Scientific research grant from The Japan Science Society, a Grant-in-Aid for Scientific Research on Priority Areas (Grant No. 11231204), a Grant-in-Aid for Scientific Research (B) (Grant No. 13555015) from the Ministry of Education, Culture, Sports, Science and Technology, the Creative and Fundamental R&D Program for SMEs, Research for the Future (RFTF) of the Japan Society for the Promotion of Science (JSPS) (JSPS–Grant No. 99P01201), and the Research Foundation for Opto-Science and Technology.

[1] D. H. Auston, K. P. Cheung, and P. R. Smith, Appl. Phys. Lett. **45**, 284 (1984).
[2] X. C. Zhang, B. B. Hu, J. T. Darrow, and D. H. Auston, Appl. Phys. Lett. **56**, 1011 (1990).
[3] K. A. McIntosh, E. R. Brown, K. B. Nichols, O. B. McMahon, K. M. Molvar, W. F. DiNatale, and T. M. Lyszczarz, Appl. Phys. Lett. **67**, 3844 (1995).
[4] K. Kawase, M. Sato, T. Taniuchi, and H. Itoh, Appl. Phys. Lett. **68**, 2483 (1996).
[5] S. L. Chuang, S. Schmitt-Rink, B. I. Greene, P. N. Saeta, and A. F. J. Levi, Phys. Rev. Lett. **68**, 102 (1992).
[6] M. Migita and M. Hangyo, Appl. Phys. Lett. **79**, 3437 (2001).
[7] S. Kono, P. Gu, M. Tani, and K. Sakai, Appl. Phys. B: Lasers Opt. **71**, 901 (2000).
[8] P. Gu, M. Tani, S. Kono, K. Sakai, and X. C. Zhang, J. Appl. Phys. **91**, 5533 (2002).
[9] H. Takahashi, A. Quema, M. Goto, S. Ono, and N. Sarukura, Jpn. J. Appl. Phys., Part 2 **42**, L1259 (2003).
[10] X. C. Zhang, Y. Liu, T. D. Hewitt, T. Sangsiri, L. E. Kingsley, and M. Weiner, Appl. Phys. Lett. **62**, 2003 (1993).
[11] C. Weiss, R. Wallenstein, and R. Beigang, Appl. Phys. Lett. **77**, 4160 (2000).
[12] H. Takahashi, Y. Suzuki, M. Sakai, S. Ono, N. Sarukura, T. Sugiura, T. Hirosumi, and M. Yoshida, Appl. Phys. Lett. **82**, 2005 (2003).
[13] M. B. Johnston, D. M. Whittaker, A. Corchia, A. G. Davies, and E. H. Linfield, J. Appl. Phys. **91**, 2104 (2002).
[14] R. McLaughlin *et al.*, Appl. Phys. Lett. **76**, 2038 (2000).
[15] J. Shan, C. Weiss, R. Beigang, and T. F. Heinz, Opt. Lett. **26**, 849 (2001).
[16] J. Heyman, P. Neocleous, D. Hebert, P. A. Crowell, T. Müller, and K. Unterrainer, Phys. Rev. B **64**, 085202 (2001).
[17] G. Meinert, L. Banyai, P. Gartner, and H. Haug, Phys. Rev. B **62**, 5003 (2000).
[18] J. R. Chelikowsky and M. L. Cohen, Phys. Rev. B **14**, 556 (1976).
[19] H. Takahashi, A. Quema, R. Yoshioka, S. Ono, and N. Sarukura, Appl. Phys. Lett. **83**, 1068 (2003).
[20] N. Sarukura, H. Ohtake, S. Izumida, and Z. Liu, J. Appl. Phys. **84**, 654 (1998).

[21] H. Ohtake, S. Ono, M. Sakai, Z. Liu, T. Tsukamoto, and N. Sarukura, Appl. Phys. Lett. **76**, 1398 (2000).
[22] H. Ohtake, H. Murakami, T. Yano, S. Ono, N. Sarukura, H. Takahashi, Y. Suzuki, G. Nishijima, and K. Watanabe, Appl. Phys. Lett. **82**, 1164 (2003).
[23] H. Takahashi *et al.*, Jpn. J. Appl. Phys., Part 2 **42**, L532 (2003).
[24] K. Watanabe, S. Awaji, M. Motokawa, Y. Mikami, J. Sakuraba, and K. Watazawa, Jpn. J. Appl. Phys., Part 2 **37**, L1148 (1998).
[25] H. Nansei, S. Tomimoto, S. Saito, and T. Suemoto, Phys. Rev. B **59**, 8015 (1999).
[26] B. R. Nag, *Electron Transport in Compound Semiconductors* (Springer, Berlin, 1980), p. 29.
[27] R. Kersting, K. Unterrainer, G. Strasser, H. K. Kauffmann, and E. Gornik, Phys. Rev. Lett. **79**, 3038 (1997).
[28] R. Kersting, J. N. Heyman, G. Strasser, and K. Unterrainer, Phys. Rev. B **58**, 4553 (1998).
[29] M. P. Hasselbeck, D. Stalnaker, L. A. Schile, T. J. Rotter, A. Stintz, and M. Sheik-Bahae, Phys. Rev. B **65**, 233203 (2002).
[30] H. Takahashi, M. P. Hasselbeck, A. Quema, M. Goto, S. Ono, and N. Sarukura, Jpn. J. Appl. Phys. Part 2 **43**, L221 (2004).